Mitigation of Cr impurity Effects

Srikanth Gopalan, Soumendra Basu, Uday Pal, and Emily Ryan
Department of Mechanical Engineering and Division of Materials Science and Engineering
&
Hossein Ghezel-Ayagh
Fuel Cell Energy

Outline

- Project objectives
- Recap of Cr poisoning mechanisms
- Role of thermodynamics and reactive transport
- Summary of ongoing work
- EPD coatings

Objectives of the project

- Systematic approach to understanding the role of thermodynamics, reactive transport leading to formation of Cr-containing reaction products, and the cell and stack operating conditions, namely, temperature, cathode gas composition, and current density.

- To propose and demonstrate solutions to mitigate or eliminate the formation of deleterious phases that are rationally based in thermodynamics, kinetics, and transport.

Mechanisms of Cr poisoning

- Hilpert et al.
  - $Cr_2O_3(s) + {}^3/_2\, O_2 \rightarrow 2CrO_3(g)$ (dry conditions)
  - $Cr_2O_3(s) + {}^3/_2\, O_2 + 2H_2O \rightarrow 2CrO_2(OH)_2(g)$ (humid conditions)

- Electrochemical reaction at cathode:
  - $2CrO_2(OH)_2(g) + 6e' + 3V_O^{\cdot\cdot} \rightarrow Cr_2O_3(s) + 3O_O^X + 2H_2O(g)$
  - $2CrO_3(g) + 6e' + 3V_O^{\cdot\cdot} \rightarrow Cr_2O_3(s) + 3O_O^X$

Mechanisms of Cr poisoning

- Cr in the gas phase and Mn in the LSM react directly to form Cr_2O_3 and eventually a manganese spinel, $(Cr,Mn)_3O_4$. The Cr_2O_3 and spinel phases that form block the transport of oxygen to the TPBs thereby decreasing the oxygen partial pressure.

- The reduced oxygen partial pressure further drives the reaction of spinel formation.

The Role of Thermodynamics

- Current density and oxygen transport in the cathode determine the oxygen partial pressure distribution, and in particular the oxygen partial pressure at the cathode/electrolyte interface.

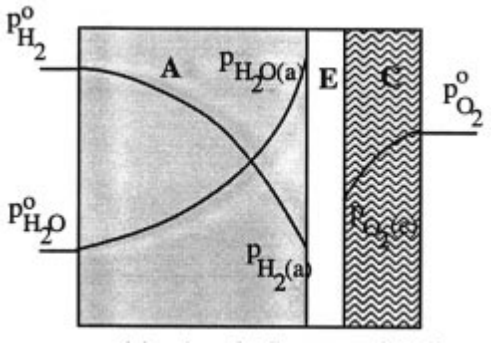

$$pO_2(c) = pO_2^0 \exp[-\frac{4F\eta_c}{RT}]$$

Introduction: The Role of Thermodynamics

- Different compounds can form depending on the temperature and local oxygen partial pressure

Perovskite cathodes	Product	More stable at	
		$p(O_2)$ (Low<0.01 atm<High)	Temperature (Low<1000K<High)
$(La_{0.8}Sr_{0.2})MnO_3$	p($La_{0.67}MnO_3$)	NA	Low
	p($LaMnO_3$)	Both (slightly low preferred)	High
	p($SrMnO_3$)	NA	High
	p($LaCrO_3$)	High	High
	$SrCrO_4$	NA	Low
	La_2CrO_6	NA	Low
	α-$SrMnO_3$	NA	Low
	p($SrMnO_{2.5}$)	Low	High
	p($SrCrO_3$)	High	High
	Mn_3O_4	Low	High
	$MnCr_2O_4$	Low	NA
$(La_{0.8}Sr_{0.2})FeO_3$	p($LaFeO_3$)	Both	Both
	p($SrFeO_{2.5}$)	Low	High
	p($LaCrO_3$)	Low	High
	Fe_2O_3	NA	High
	$SrCrO_3$	Mid-range	High
	$SrFe_{12}O_{19}$	Both	Both
	$SrCrO_4$	High	Low
$La(Ni_{0.6}Fe_{0.4})O_3$	p($LaNiO_3$)	High	Both
	p($LaFeO_3$)	Both	Both
	NiO	Low	High
	La_2NiO_4	NA	High
	p($LaCrO_3$)	Both	Both
	$La_4Ni_3O_{10}$	Low	High

Summary of project tasks and overview of ongoing work

- Electrochemically testing symmetrical and full cells with exposure to Cr_2O_3 in a dry and humid atmosphere as a function of pH_2O (cathode), temperature, cathode microstructure, thickness, and current density.
- Microstructural and TEM/FIB analysis of tested cross-sections.
- Mapping of reaction products with pH_2O (cathode), temperature and current density.
- Computational modeling.
- Development of protective coatings

Schematic of electrochemical cell

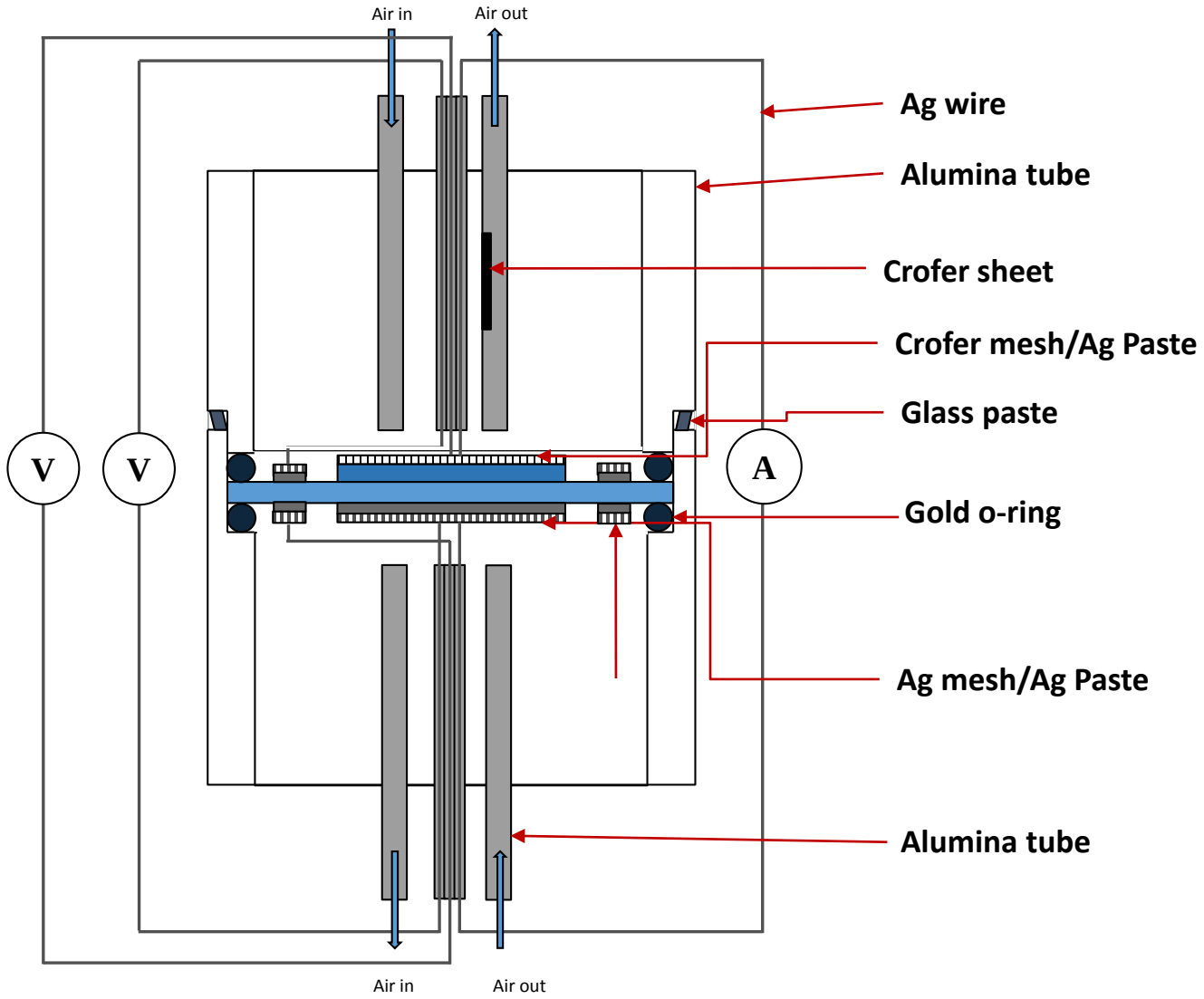

SEM image of cathode cross section (1200°C)

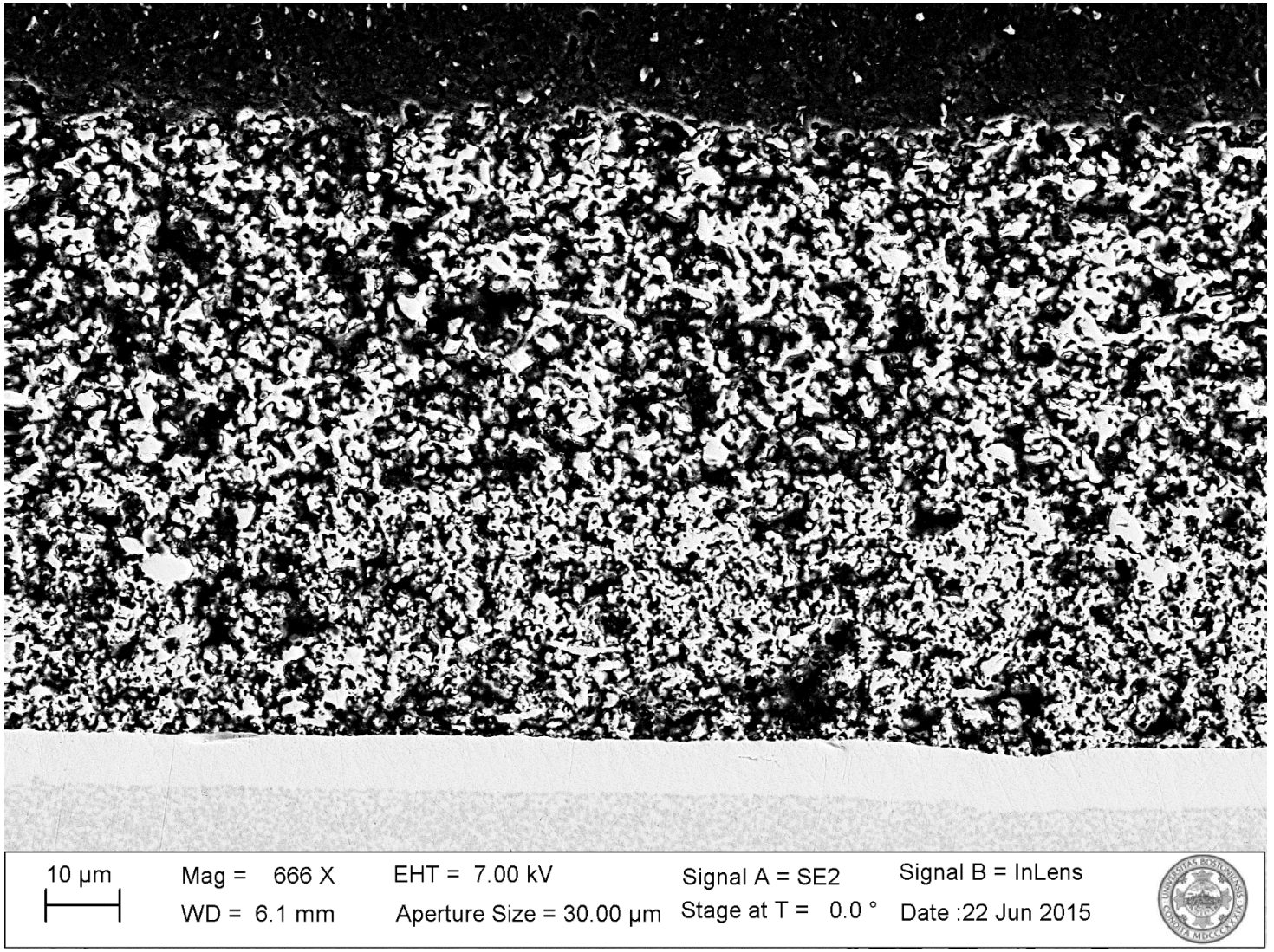

CCCL, 51.525 µm,
Porosity: 49.74%

CAL, 34.068 µm,
Porosity: 36.70%

YSZ, 7.672 µm

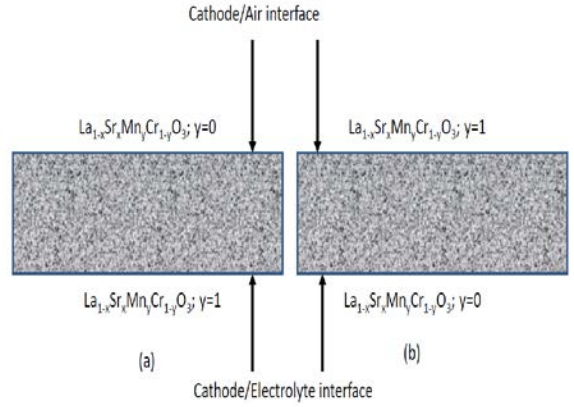

Computational Investigations of Chromium Poisoning

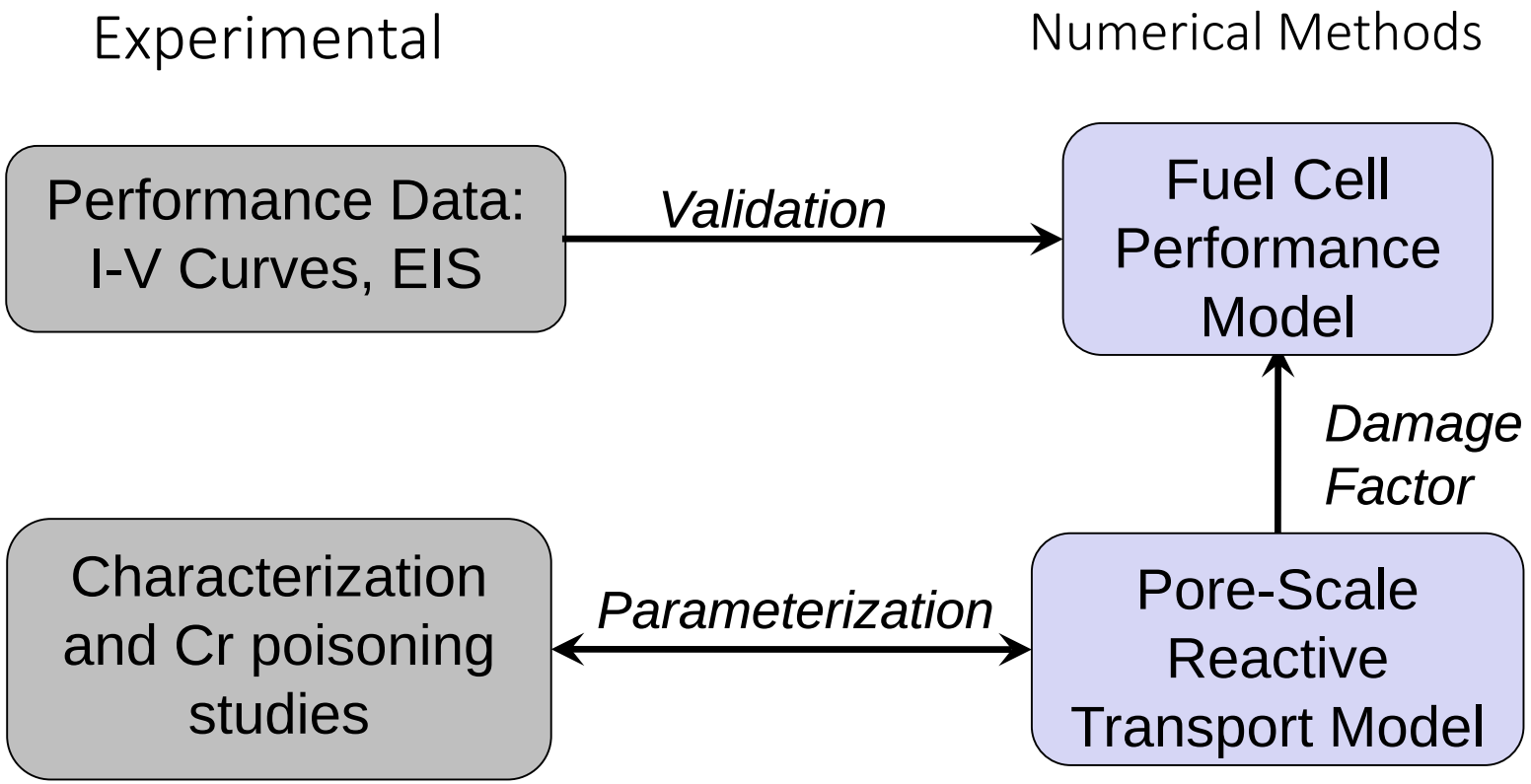

Pore-Scale Reactive Transport Model

- Develop a small scale model of reactive transport in the porous cathode
- Model will resolve cathode micro-structure
- Formulate a damage factor to include Cr poisoning in full cell performance model

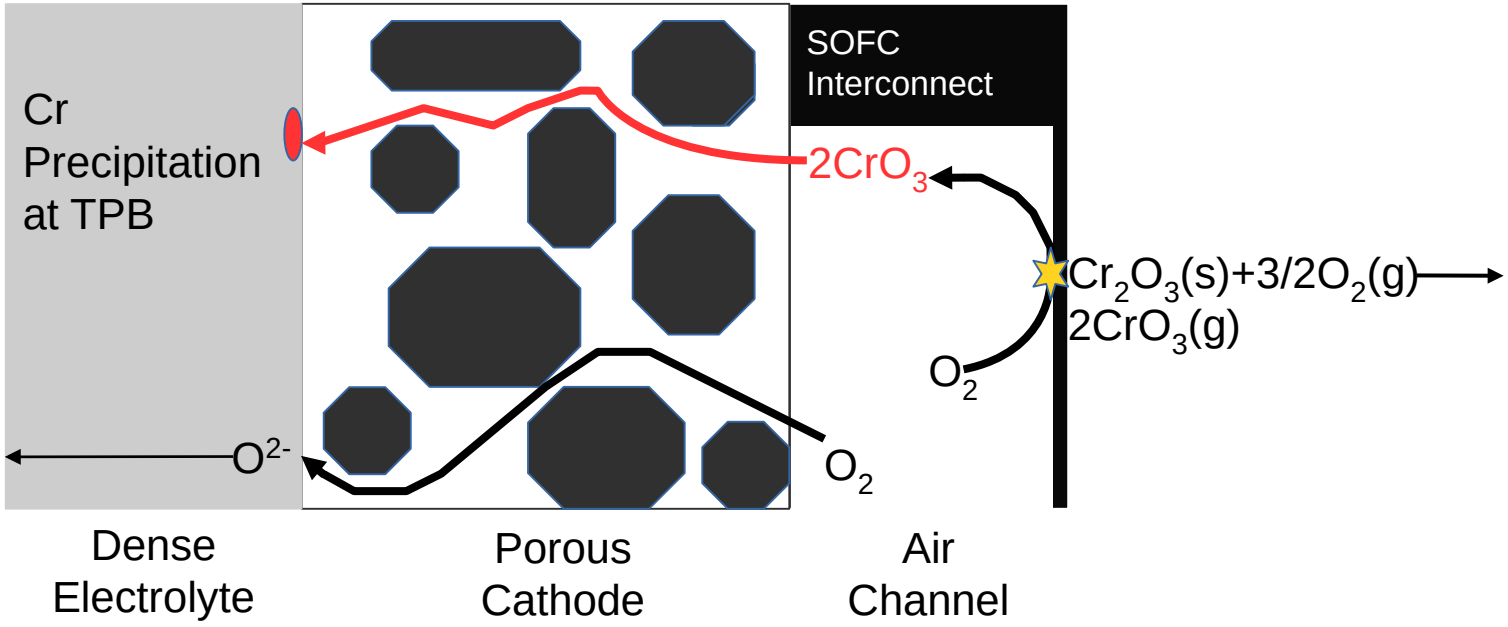

BU Approach to Protective Coatings using EPD

Requirements of Protective Coatings

- Adherence with the substrate
- Stability (Thermodynamic & Thermomechanical)
- High electronic conductivity
- Low oxygen ion conductivity
- Spallation resistance (thermal cyclability)

Prior Candidates and Application Methods

- A number of spinel and perovskite coatings – e.g. $(Mn,Co)_3O_4$, $(Mn,Cr)_3O_4$, $La_{1-x}Sr_xMnO_3$, $LaMn_{0.9}Ti_{0.1}O_3$, $La_{1-x}Sr_xCrO_3$ etc.

- Atmospheric plasma spray (APS), aerosol deposition followed by sintering, sputtering, PVD etc.

- Principle issues have been adhesion to substrate, high density of coatings, and spallation of coatings after long term operation of cells.

BU Approach

- Using a cost effective process-Electrophoretic Deposition (EPD) to apply a dense $CuMn_{1.8}O_4$ spinel oxide on Crofer 22 APU to reduce the oxidation of the alloy, minimize chromium transport and attack, and maintain a low interfacial resistance

Properties of $CuMn_{1.8}O_4$ Spinel

- Electrical conductivity of $CuMn_{1.8}O_4$ at 800 C is around 100S/cm

Material	Thermal expansion coefficient /K
$CuMn_{1.8}O_4$	12.2×10^{-6}
Crofer 22 APU	12.0×10^{-6}
LSM	12.0×10^{-6}
YSZ	11.0×10^{-6}

Electrophoretic Deposition Schematic

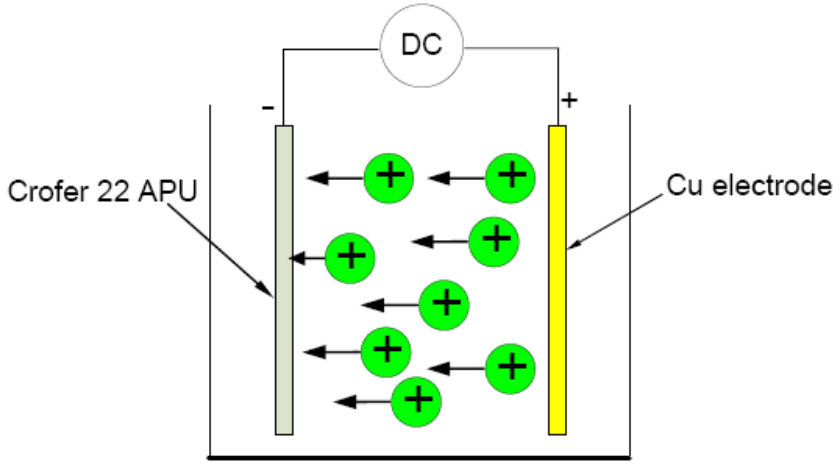

Coating Process

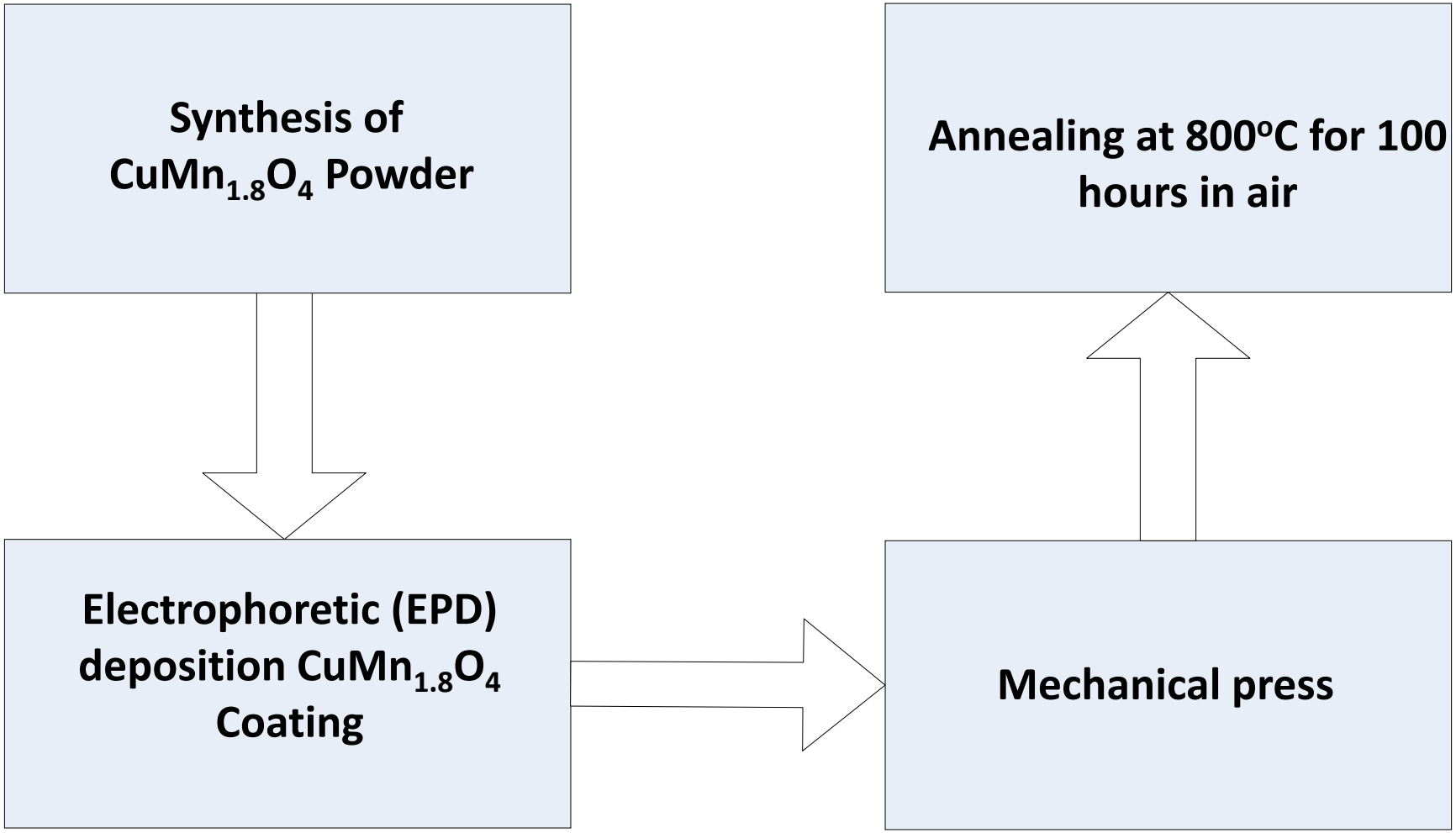

XRD of Coated and Uncoated Crofer 22 APU

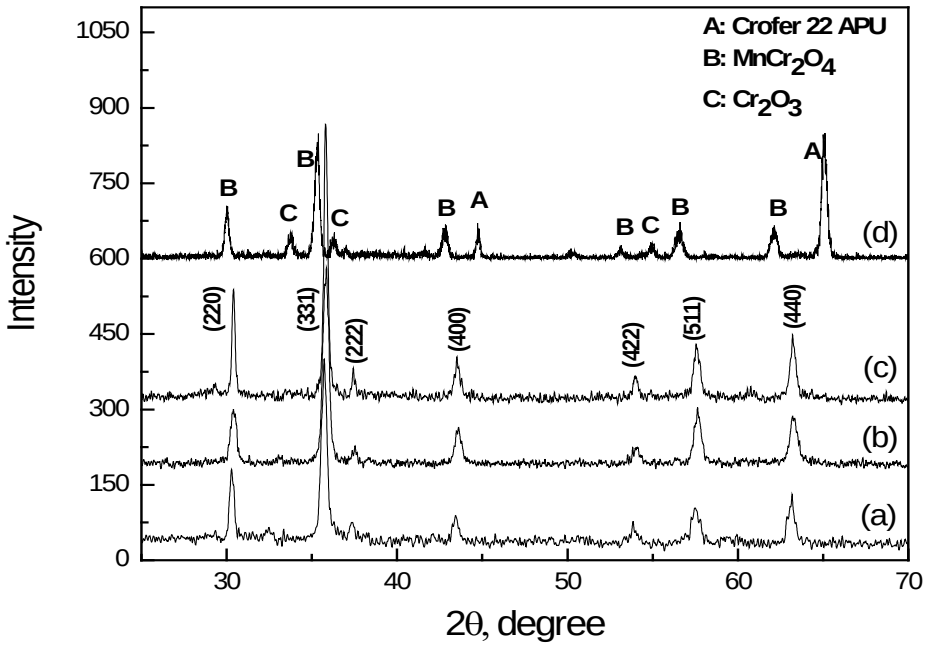

(a)As-deposited $CuMn_{1.8}O_4$ coating sample,
(b)Coated sample after 800c 100h annealing
(c)Coated sample (b) after 800C 100h isothermal oxidation
(d)Uncoated sample after 800C 200h isothermal oxidation

Cross-Sectional SEM of Coated Sample

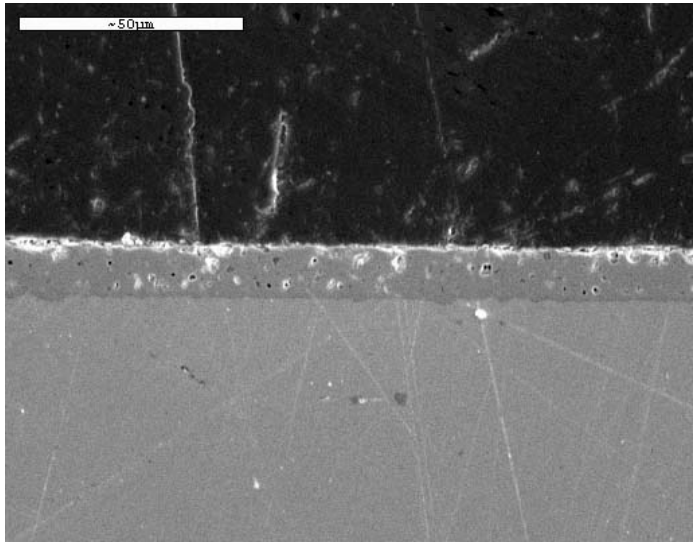

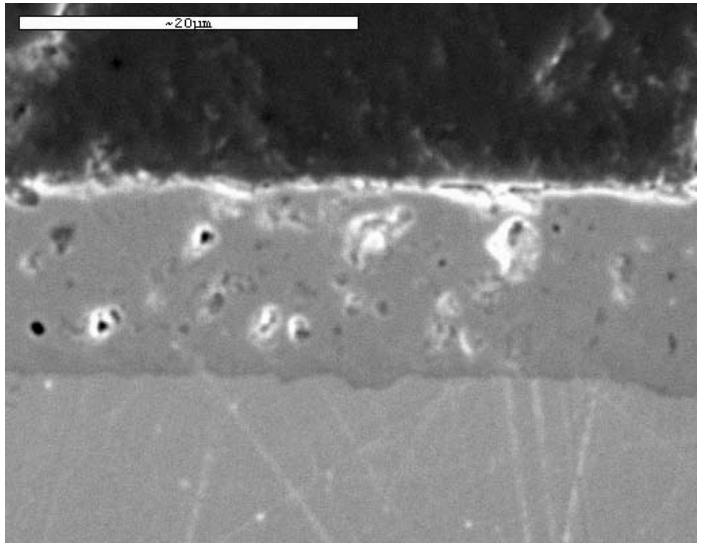

Weight Gain of Uncoated and Coated Samples

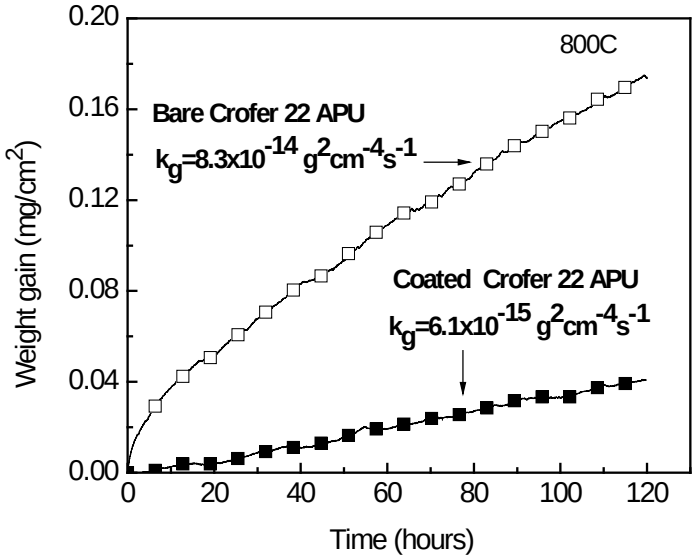

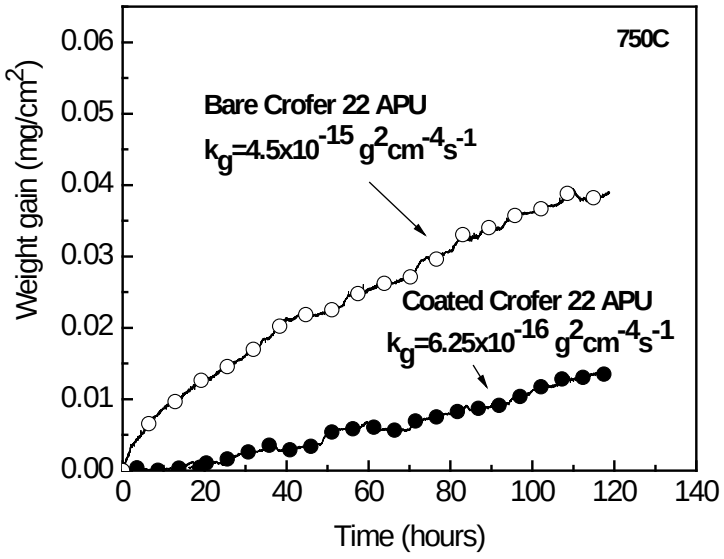

Oxidation Rate Parameters for Uncoated and Coated Samples

	Oxidation temperature (°C)	k_g ($g^2\ cm^{-4}\ s^{-1}$)	k_p ($\mu m\ h^{-1/2}$)	Oxide thickness after 50000 h (μm)
Uncoated Crofer 22 APU	800	8.3×10^{-14}	10.51×10^{-2}	**23.5**
	750	4.5×10^{-15}	2.45×10^{-2}	5.5
Coated Crofer 22 APU	800	6.1×10^{-15}	2.87×10^{-2}	**6.4**
	750	6.25×10^{-16}	1.06×10^{-2}	2.4

$$k_p = 6 \times 10^5 \left[\frac{MW_{Cr_2O_3}}{(3/2) MW_{O_2}} \frac{1}{\rho_{Cr_2O_3}} \right] \sqrt{k_g}$$

Elemental Distribution Map of Uncoated Sample after 800 °C, 120 h Isothermal Oxidation

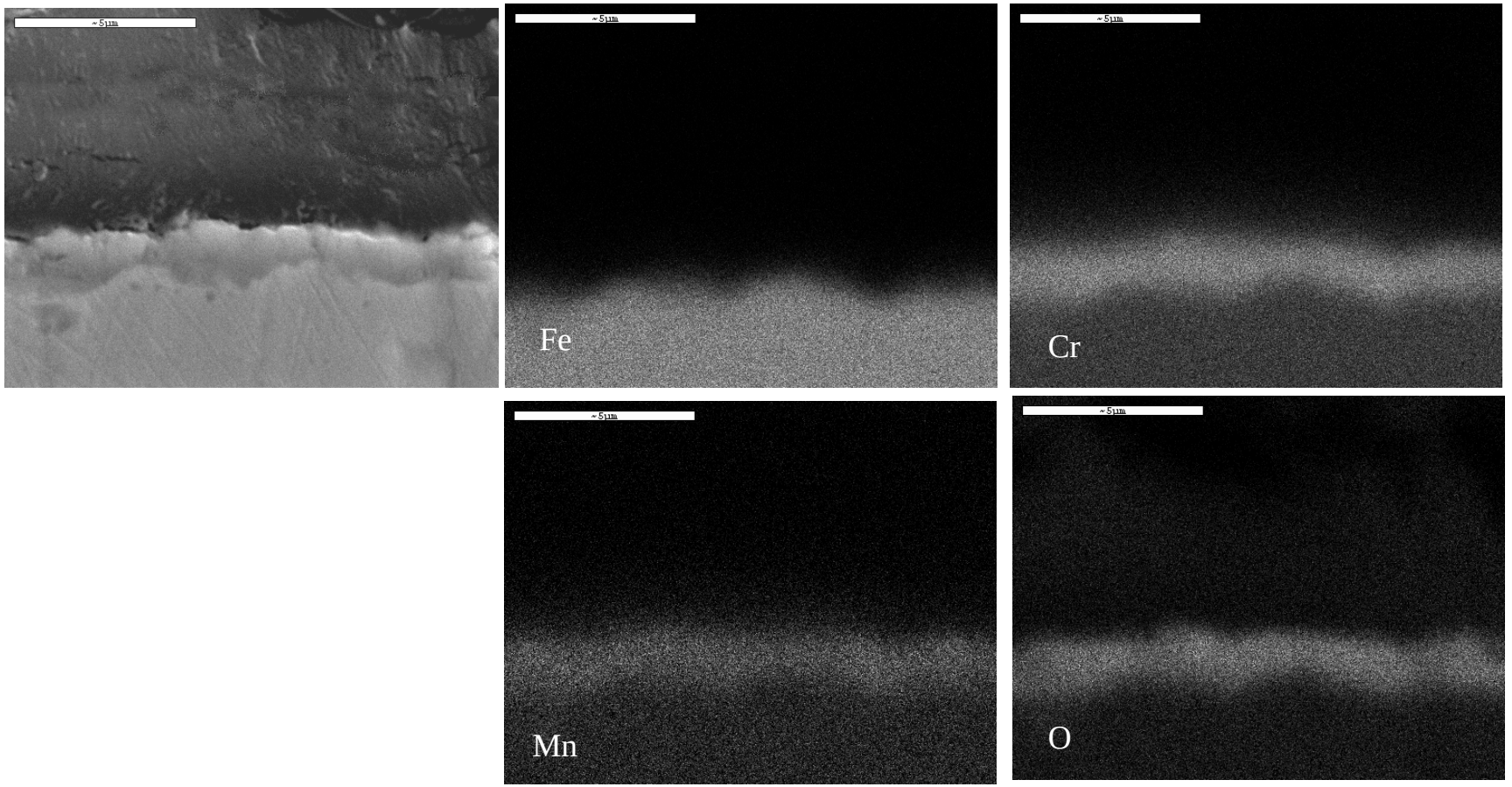

Elemental Distribution Map of Coated Sample after 800 °C, 120 h Isothermal Oxidation

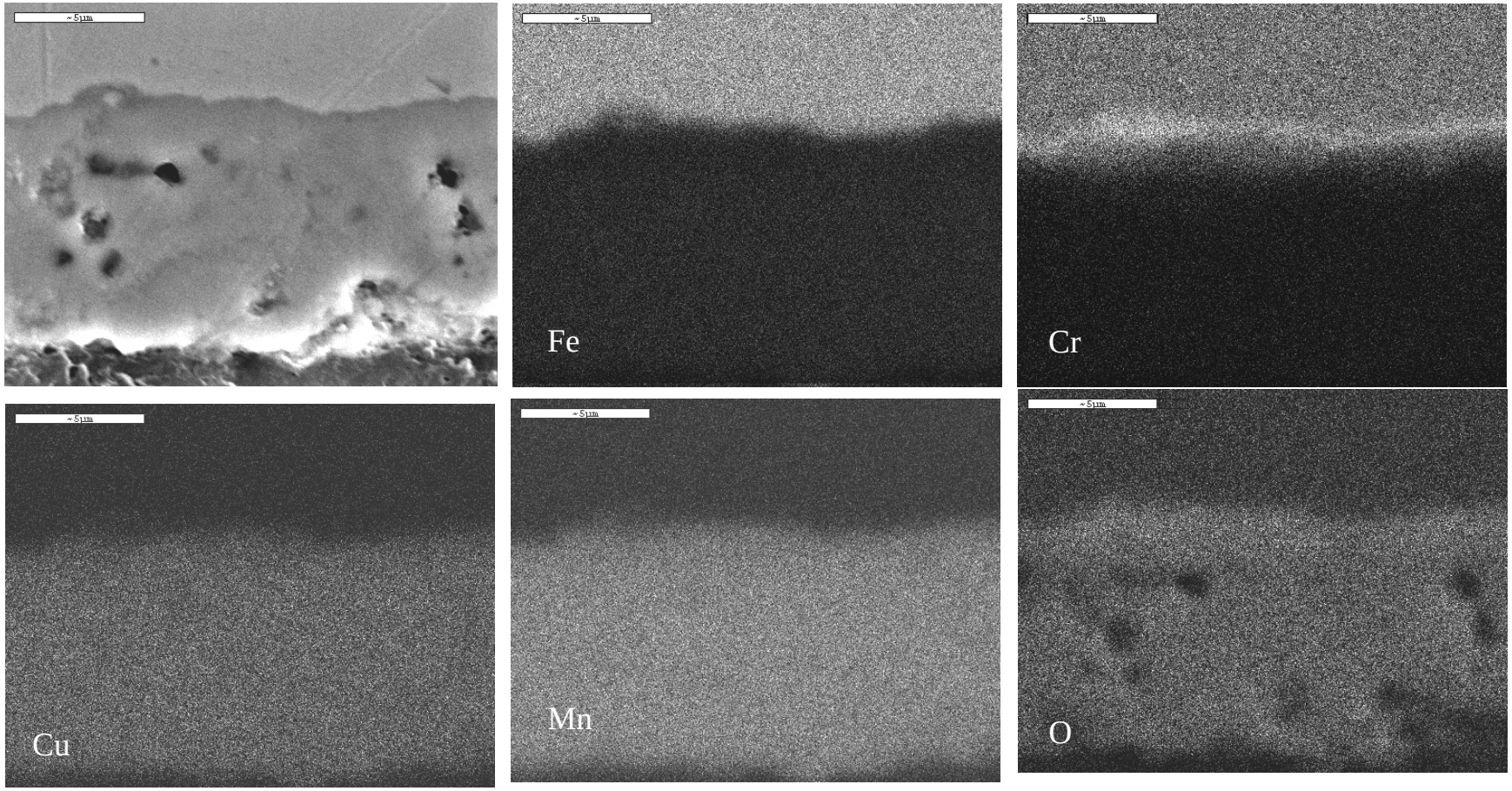

Schematic structure of oxide layer

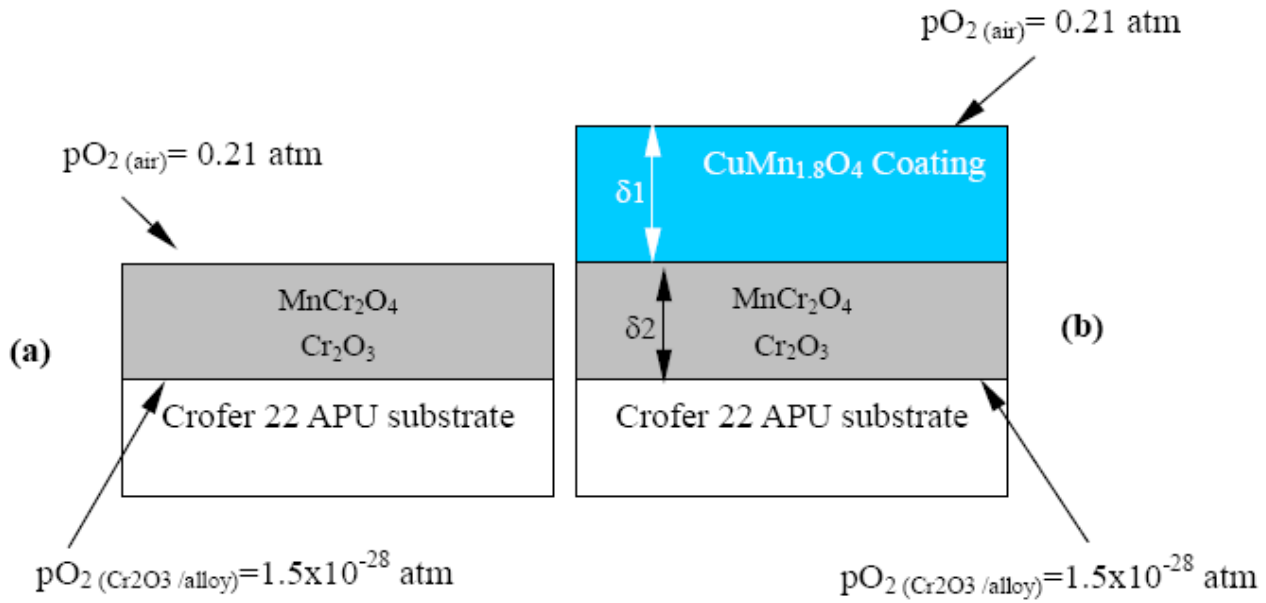

(a) Uncoated Crofer 22 APU (b) Coated Crofer 22 APU

Transport Model – Converting flux equations to rate of oxide layer growth

Flux due to chemical and electrostatic potential gradients:

$$j_{Cr^{3+}} = -\frac{\sigma_{Cr^{3+}}}{Z_{Cr^{3+}}^2 F^2}\left(\frac{d\mu_{Cr^{3+}}}{dx} + 3F\frac{d\Phi}{dx}\right)$$

$$j_{O^{2-}} = -\frac{\sigma_{O^{2-}}}{Z_{O^{2-}}^2 F^2}\left(\frac{d\mu_{O^{2-}}}{dx} - 2F\frac{d\Phi}{dx}\right)$$

$$j_n = -\frac{\sigma_n}{Z_n^2 F^2}\left(\frac{d\mu_n}{dx} - F\frac{d\Phi}{dx}\right)$$

Electroneutrality condition:

$$Z_{Cr^{3+}} j_{Cr^{3+}} + Z_{O^{2-}} j_{O^{2-}} + Z_n j_n = 0$$

$$\left|j_{Cr_2O_3}\right| = \left|\frac{1}{12}\left[\frac{\sigma_n(\sigma_{O^{2-}} + \sigma_{Cr^{3+}})}{F^2(\sigma_{O^{2-}} + \sigma_{Cr^{3+}} + \sigma_n)}\right]\frac{d\mu_O}{dx}\right|$$

Oxide growth rate ($\frac{d\delta}{dt}$)

Effective diffusivity (D)

Oxygen partial pressure gradient ($\frac{d\ln pO_2}{dx}$)

Combining:

$$\frac{d\Phi}{dx} = \frac{1}{6}\left[\frac{3\sigma_{O^{2-}}\frac{d\mu_{O^{2-}}}{dx} + 6\sigma_n\frac{d\mu_n}{dx} - 2\sigma_{Cr^{3+}}\frac{d\mu_{Cr^{3+}}}{dx}}{F(\sigma_{O^{2-}} + \sigma_{Cr^{3+}} + \sigma_n)}\right]$$

$$\frac{d\delta}{dt}\frac{1}{D}dx = d\ln(pO_2)$$

Transport Model – Converting flux equations to rate of oxide layer growth

$$2Cr + 3/2O_2 \rightarrow Cr_2O_3$$

$$\Delta G = -1{,}120{,}300 + 260T \text{ J mol}^{-1} \text{ K}^{-1}$$

pO_2 at alloy/Cr_2O_3 interface can be calculated from the above data and used in integrating oxide layer growth rate equation

$$\frac{d\delta_2}{dt} = \frac{\Delta \ln(pO_2)}{\frac{\delta_1}{D_1} + \frac{\delta_2}{D_2}} = \frac{a}{b + \delta_2}$$

$$a = D_2 \Delta \ln(pO_2) \text{ and } b = \delta_1 D_2 / D_1$$

$$\frac{\delta_2}{2\Delta \ln(pO_2)\frac{D_2}{\delta_2}} + \frac{\delta_2}{\Delta \ln(pO_2)\frac{D_1}{\delta_1}} = t + \tau$$

- Initial stage – scale thickness small; growth rate dominated by transport through coating, linear kinetics
- Later stage – scale thickness large; growth rate dominated by transport through scale, parabolic kinetics.
- Intermediate stage – transition regime, paralinear kinetics

Data Analysis

	Oxidation temperature (C)	K_g (g^2/cm^4s)	D_1 (cm^2/s)	D_2 (cm^2/s)	Total oxide thickness (μm)
Uncoated Crofer 22 APU	800	$6.67X10^{-14}$	NA	$2.5X10^{-16}$	1.1
	750	$3.64X10^{-15}$	NA	$1.6X10^{-17}$	0.55
Coated Crofer 22 APU	800	NA	$2.0X10^{-15}$	$2.5X10^{-16}$	0.7
	750	NA	$5.0X10^{-16}$	$1.6X10^{-17}$	0.25

δ_1/D_1 and δ_2/D_2 are the contributions of diffusion resistances from coating and scale

Based on our analysis of the data:
Equal contributions from coating and scale occurs at 850 h at 800^{o}C
Equal contributions from coating and scale occurs at 100 h at 750^{o}C

Our measurements at both temperatures were for 120 h. Thus 800^{o}C data follow linear kinetics and 750^{o}C data follow paralinear kinetics

Schematic of ASR measurement setup

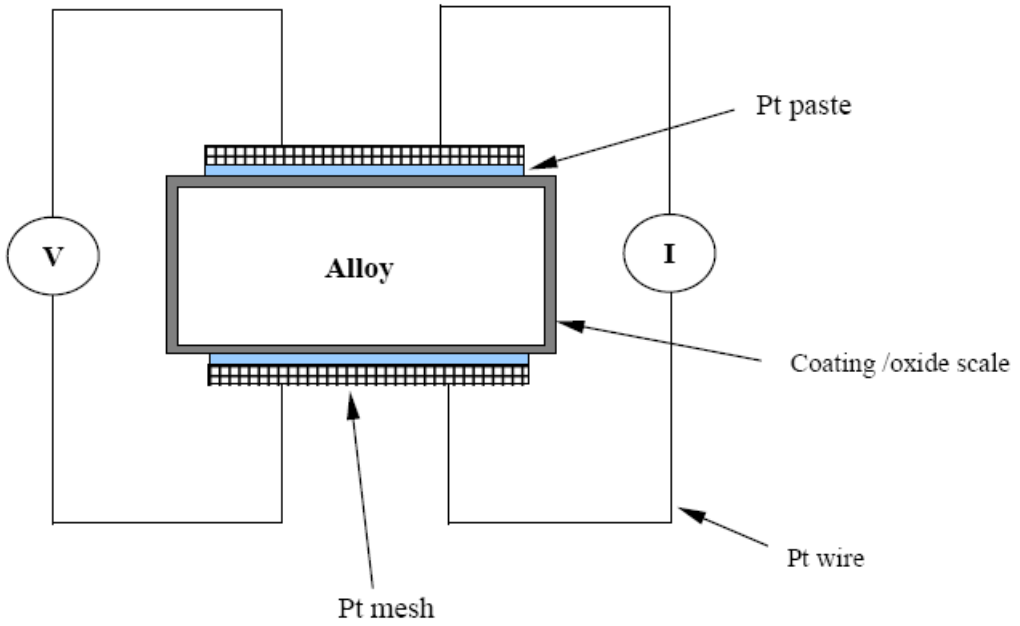

ASR as a function of temperature for the various samples

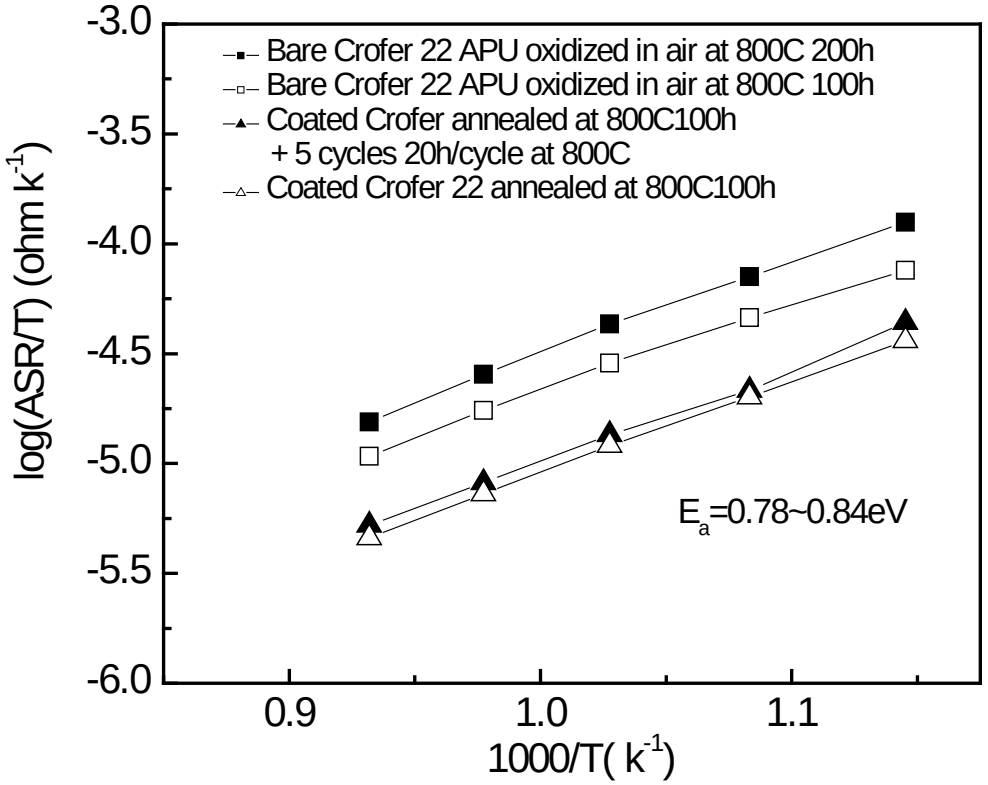

Predicted long time ASR

	temperature (°C)	Oxide thickness after 50000 h (μm)	Resistivity of Cr_2O_3 (mΩcm)*	ASR after 50000 h ($m\Omega cm^2$)
Coated Crofer 22 APU	800	6.4	$1.7x10^4$	11
	750	2.4	$2x10^4$	4.8

* W. Qu, etc, J. Power Sources, 153(1), 114 (2006)

Target Interconnect ASR $\leq 100 m\Omega cm^2$

Future work on coatings

- Other materials compositions to be explored through EPD technique
- Transport in newer coating materials can be altered by suitable doping strategies and engineering the point defect structure

Acknowledgments

- DOE personnel -- Steven Markovich, Rin Burke, Shailesh Vora

- Wenhua Huang – Former graduate student (EPD coatings work)